INTERNATIONAL JOURNAL OF INTEGRATED ENGINEERING
ISSN: 2229-838X e-ISSN: 2600-7916

IJIE

Vol. 16 No. 7 (2024) 300-312
https://publisher.uthm.edu.my/ojs/index.php/ijie

Structural Design and Motion Analysis of Reconfigurable Tracked Pipeline Robot

Jia Chaoyu[1,2], Wan Nurshazwani Wan Zakaria[1]*, Chen Pengwei[2], Nor Azmi Bin Ab Patar[1]

[1] [1]*School of Mechanical Engineering, College of Engineering*
Universiti Teknologi MARA, 40450 Shah Alam, Selangor, MALAYSIA

[2] *Shaanxi Polytechnic Institute, Xianyang*
Xianyang, 712000, Shaanxi, CHINA

*Corresponding Author: wshazwani@uitm.edu.my
DOI: https://doi.org/10.30880/ijie.2024.16.07.027

Article Info

Received: 27 June 2024
Accepted: 17 November 2024
Available online: 31 December 2024

Keywords

Reconfigurable structure, pipeline robot, active diameter-changing mechanism, motion analysis

Abstract

There has been a renewed interest in development of pipeline robot to meet the demand of regular inspection and maintenance. This paper focuses on structural design and motion analysis of the developed reconfigurable tracked pipeline robot. The robot features an active diameter-changing mechanism, and an independent control drive module allowing it to adjust its tracks to fit the inner wall size of circular pipelines during manoeuvring. A comprehensive dynamic motion analysis was conducted to determine the necessary motion and force for effective robot movement. Both simulation and experimental tests were performed in horizontal and sloping pipelines. It was found that the angular velocity is relatively stable and reciprocating within a range of -2.7 to 1.7 °/s. The simulation results exhibit that the robot has good adaptability to pipeline sizes which demonstrate that the robot performs effectively within circular pipelines.

1. Introduction

The water supply pipeline system is a vital part of the municipal infrastructure which provide safer and continuous transportation of fresh water to the residential area. However, the freshwater pipelines are prone to issues such as leaks, blockage and malfunctioning devices [1]. It is necessary to perform regular maintenance and inspections. Therefore, timely and effective inspection of the pipeline system is very important.

In conventional pipeline inspections, human inspectors perform all detection tasks, including visual assessment, sounding, and tapping, which poses certain risks and results in labor-intensive, time-consuming, and ineffective detection efficiency, particularly in hard-to-reach or buried sections [2]. In recent years, pipeline detection robots have gained renewed interest due to the growing demand for pipeline inspection and maintenance, where can address a critical challenge in the pipeline industry [3-5].

The pipeline inspection robot is a mechanical device that integrate various sensors, intelligent mobile carriers, operating devices, and non-destructive testing technologies to enter complex and ever-changing unstructured pipeline environments that humans cannot reach, completing tasks such as inspection, cleaning, and maintenance [6-8]. With the development of machine learning, pattern recognition, and neural networks, the research on intelligent behaviour of robots has been elevated to the next advancement of robot system development [9-10].

Nevertheless, structural design and mechanism of the robot is very important to ensure robot maneuverability in pipeline confined space. A number of researchers have developed different types of pipeline robots. The Versatrax series pipeline robots from Inuktun adopts a tracked system that has a unique mechanism which can change the structure and size according to the shape and size of the pipeline [11]. Hui Li [12] designed

a detection robot consists of three sets of symmetrical support wheels. Each spring mechanism is connected between a fixture and a motion component, to compose a compliant mechanism that connects each wheel and chassis. Xiaomin Liu [13] developed a worm inspired soft robot that can operate and perform various tasks in complex pipeline/tunnel environments. The soft tubular robot consists of elongation pneumatic actuators (EPAs), radial expansion pneumatic actuators (REPAs), and a spatial bending pneumatic actuator (SBPA). Guanhua Feng [14] proposed a novel wheeled and wall-pressing type in-pipe cleaning robot (IPCR) with high pressure water jet.

Kim et al. [15] and Tourajizadeh et al. [16] have conducted relevant studies on the motion route and control of pipeline robots. Yan Hongwei et al. [17] designed a fully driven wheeled pipeline robot and studied the dynamic characteristics of the robot during cornering. Abidin et al, [18] conducted research on the pass-ability of tracked pipeline robots. Zhao Wentao et al. [19] conducted research on the structural design and dynamic characteristics of pipeline robots. Based on the comprehensive consideration of pipeline environment and robot walking mode, this project chooses an electric push rod variable diameter tracked pipeline robot.

2. Methodology

2.1 Design of Pipeline Robot Mechanism

Fig. 1 shows the proposed pipeline robot mechanism consists of a driving module, a supporting structure, a variable diameter mechanism, a CCD camera, and a light source for imaging system. The driving module provides power for the robot to walk in a circular pipeline.There are three sets of driving modules which are arranged evenly along the circumference at an angle of 120 degrees. Drive modules consist of servo motors, reducers and synchronous belt transmission mechanisms. The motion of each of these units can be controlled independently.

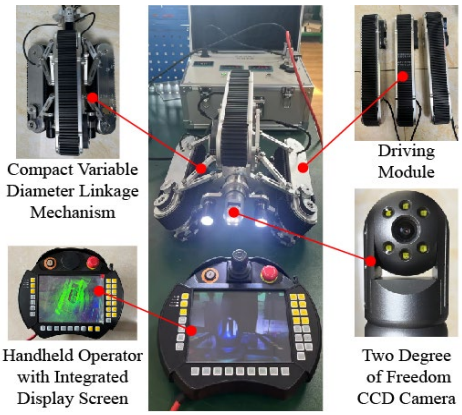

Fig. 1 *Overview of the pipeline robot system*

The variable diameter mechanism consists of a servo motor, a screw, and a connecting rod mechanism. It works on the principle of driving the ball screw to rotate through a coupling, which then drives the screw nut to undergo linear reciprocation. A connecting rod mechanism is used to adjust the outer diameter of the three sets of driving modules by changing the support angle to adjust the outer diameter of the connecting rod mechanism, allowing the driving module track to remain in contact with the pipeline interior wall regardless of the changes in the pipeline internal diameter.

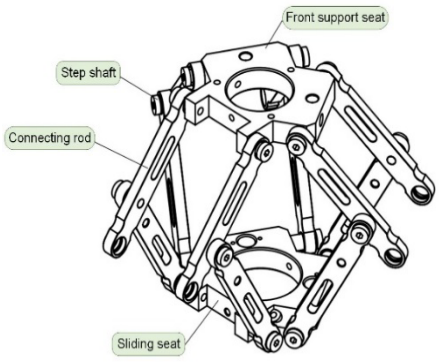

Fig. 2 *Connecting rod variable diameter mechanism*

The pipeline robot is designed to be capable of adapting to pipe diameters ranging from 300 to 420mm. Using three independent driving modules, the robot can adapt to circular pipes of different sizes due to its reconfigurable mechanism. For real-time pipeline detection operations, the equipped CCD camera can transmit real-time images inside the pipeline. The robot body is made of aluminum alloy material, with an axial length of 400 mm and a mass of 19.8 kg. The motor power of the variable diameter mechanism is 60 W, and the motor power of a single drive module is 60 W. The speed ratio of the drive module reducer is 1:5. The single drive module can provide a traction force of 122 N, and the total traction force of the robot is 366 N. The rated maximum operating speed of the robot is 1140 mm/s, and the experimental speed is 200 mm/s.

2.2 Pipeline Robot Dynamic Characteristic Analysis

This section concentrates on simulated motion analysis due to the motion changing behaviour of reconfigurable track to provide insights into dynamic behaviour and performance of the robot during maneuver task. The simulation is conducted using MATLAB R2016a and Adams 2016 software.

The angle between the wheel system of the robot in contact with the top of the pipeline and the center line in the direction of gravity is defined as β in which is configured as 0°≤β≤120°. G represents the robot's gravity, N_1, N_2, and N_3 represent the positive pressure exerted by the inner wall of the pipeline on the three main driving wheels of the robot [20-21]. The pose and force analysis of the robot inside the pipeline are shown in Fig. 3.

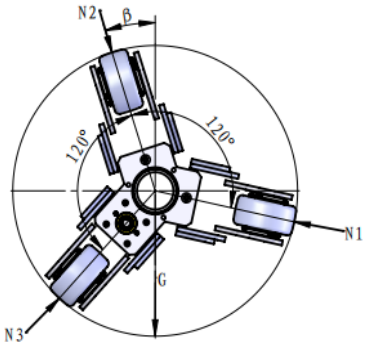

Fig. 3 *Position and force analysis of robot inside pipelines*

The force balance conditions are given as Equation 1:

$$\begin{cases} N_2 \sin\beta + N_1 \cos\beta + N_3 \cos(60° - \beta) = 0 \\ N_2 \cos\beta + N_1 \sin(30° - \beta) + N_3 \cos(60° - \beta) = \frac{G}{2} \\ F = \sum_{i=1}^{3} \varphi(N_i + N_{i2}) = \sum_{i=1}^{3}(F_i + F_{i2}) = \frac{\sum_{i=1}^{3} M_i}{r} \\ G\cos\beta + 3N_0 = \sum_{i=1}^{3}(N_i + N_{i2}) \end{cases} \quad (1)$$

where M_i outputs torque to the main drive wheel system.

The output torque can be calculated as Equation 2 as the robot rotates in the pipeline (around the z-axis direction) :

$$T - R\sum_{i=1}^{3} \mu(N_i + N_{i2}) = Ja_t \quad (2)$$

μ is the coefficient of rotational friction.

The total traction force F, F_i and F_{i2} of the robot's motion are the traction forces of the active and passive driving wheels of the robot in contact with the pipe wall. r is the radius of rotation of the driving wheel and m is the mass of the robot. The robot is placed in a horizontal pipeline, and T is the rotational torque caused by the

deviation of the robot's center of gravity in the pipeline. R is the radius of rotation of the robot. J is the moment of inertia of the robot and α_t is the angular acceleration of the robot's rotation.

The torque of the driving motor of the robot's variable diameter mechanism is M_0, which generates the same thrust on the three sets of driving modules, so that the pressure generated by the contact between the wheel and the pipe wall of the three sets of driving modules is N_0. M_i acquires the data through the working mode of the servo motor, so that the positive pressure N_i of the contact between the driving wheel and the pipe wall of the robot and the total traction force F, T, and J of the robot's movement can be obtained when the robot is running in the pipeline. The total values of traction force F, T, and J of the robot's movement need to satisfy β angular conditions. The motion characteristics of the robot rotating in the pipeline can be obtained by measuring and solving for α_t using simultaneous equations (1) and (2).

Fig. 4 shows the robot configuration inside the pipeline slope. The slope angle of the pipeline is defined by θ ($0° \le \theta \le 90°$).

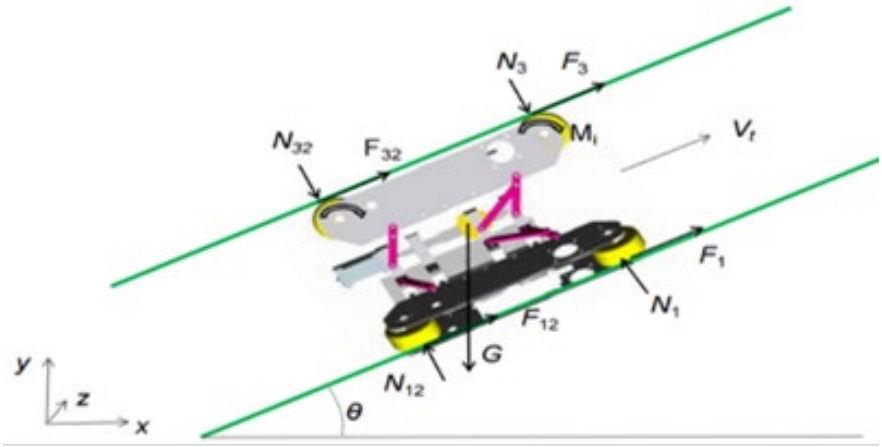

Fig. 4 *Position and force analysis of robot inside pipeline slope*

$$\begin{cases} N_2 \sin\beta + N_1 \cos\beta + N_3 \cos(60° - \beta) = 0 \\ N_2 \cos\beta + N_1 \sin(30° - \beta) + N_3 \cos(60° - \beta) = \dfrac{G \cos\theta}{2} \\ F = \sum_{i=1}^{3} \varphi(N_i + N_{i2}) = \sum_{i=1}^{3} (F_i + F_{i2}) = \dfrac{\sum_{i=1}^{3} M_i}{r} \\ G \cos\beta \cos\theta + 3N_0 = \sum_{i=1}^{3} (N_i + N_{i2}) \end{cases} \tag{3}$$

The output force can be calculated as Equation 4 as the robot moves along the pipeline:

$$F - G \sin\theta - \sum_{i=1}^{3} \mu(N_i + N_{i2}) = m\dot{V}_t \tag{4}$$

V_t can be calculated by solving equations (3) and (4) simultaneously, which represents the motion characteristics of the robot in a horizontal pipeline.

2.3 Analysis of Pipeline Robots during Climbing in Vertical Pipeline

During robot movement, the electric push rod in the middle of the robot will contract, which causes three sets of linkages to rotate, thereby making the driving module adhere tightly to the inner wall of the pipeline. It is possible for the robot to exert sufficient pressure on the inner wall of the pipeline when it moves vertically along the

Int. Journal of Integrated Engineering Vol. 16 No. 7 (2024) p. 300-312

pipeline, thereby preventing the exhibit friction force of the robot from sliding down or being unable to climb the vertical direction [22].

To determine the minimum pressure that the robot must provide to the inner wall of the pipeline in the vertical direction, the relationship between the pressure on the inner wall of the pipeline within the diameter range that the robot can adapt to and the robot's structural parameters is analyzed [23]. Fig. 5 shows the stationary state of the robot inside the vertical pipeline which is subjected to its own gravity G. The diameter changing mechanism provides two pressures F_{N1} and F_{N2} to the two front and rear track wheels, N_1 and N_2 is the pressure provided by the inner wall of the pipeline to the two wheels, and the F_{f1} and F_{f2} represents the friction force between the inner wall of the pipeline and the two wheels. The friction coefficient between the inner wall of the pipeline and the track is μ. R is the radius of the robot's wheels, L is the center distance between two track wheels, H_0 is the shortest vertical distance from the center of the track wheel to the extension line of the robot's center of gravity when the maximum diameter range is 400 mm. The weight of the pipeline robot with sensors is less than 20 kg, resulting in a robot gravity of G = 196 N.

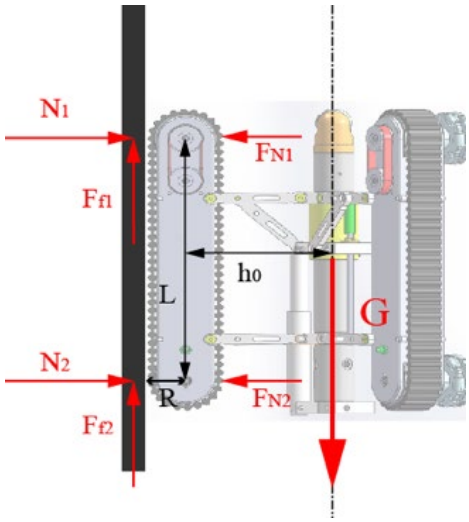

Fig. 5 *Critical state force analysis of robot in vertical configuration*

The static equilibrium Equation 3 of the robot in this state can be obtained:

$$\begin{cases} F_{f1} + F_{f2} - \frac{1}{3}G = 0 \\ F_{f1} = \mu N_1 \\ F_{f2} = \mu N_2 \\ N_1 + N_2 = F_{N1} + F_{N2} \\ -N_1 L + F_{N1} L = 0 \\ N_2 L - F_{N2} L = 0 \\ -(F_{f1} + F_{f2})R + N_2 L - F_{N2} L - \frac{1}{3}Gh_0 = 0 \end{cases} \quad (5)$$

When the robot is in the state shown in Fig. 4, its wheels are subjected to pressure N_1 and N_2 from the inner wall of the pipeline, as well as pressure F_{N1} and F_{N2} from the support plate of the variable diameter mechanism. By analyzing the force on this condition, it can be concluded that the torque of F_{N1} and N_1 to the center of the other wheel is equal in magnitude and opposite in direction. Same condition applies to the torque of F_{N2} and N_2. Considering both set of forces are centered at L, according to the static equilibrium of Equation 5, F_{N1}=N_1 and F_{N2}=N_2 can be obtained as Equation 6:

$$\begin{cases} F_{f1} + F_{f2} - \frac{1}{3}G = 0 \\ F_{f1} = \mu N_1 \\ F_{f2} = \mu N_2 \\ N_1 + N_2 = F_{N1} + F_{N2} \\ -(F_{f1} + F_{f2})R - \frac{1}{3}Gh_0 = 0 \end{cases} \quad (6)$$

The total forces (F_{N1}+F_{N2}) can be obtained by solving the static equilibrium of Equation 6 yields:

$$F_{N1} + F_{N2} = -\frac{Gh_0}{3\mu R} \quad (7)$$

By substituting the structural parameters of the robot into Equation 7, the minimum value of (F_{N1}+F_{N2}) can be obtained as 326.7 N. At this limit state, the three radially uniformly distributed driving modules need to provide three times the positive pressure on the inner wall of the pipeline as the driving module in a single direction, so F_N=3 and (F_{N1}+F_{N2}) =980 N. By analyzing the critical state of robot in vertical pipeline, a foundation can be laid for the subsequent production of robot physical prototypes and optimization of variable diameter mechanisms.

2.4 Passability Analysis of Pipeline Robot in Elbow Pipe

Robot may encounter a variety of complex situations, including turns, obstacles and changes in pipe diameter during operation. A pipeline robot's ability to corner, cross obstacles, and change diameter is an important indicator for judging its performance. Thus, the passability analysis of robots is conducted inside L-shaped pipe from both theoretical and experimental perspective.

An example of a common working scenario for pipeline inspection robots is the inspection of pipelines buried underground in cities, which must comply with the work conditions of linear motion and turning motion of horizontal pipelines. As an example, Fig. 6 illustrates how a robot can smoothly pass through a 90° elbow pipe. A theoretical analysis of the robot's size is presented, and the cornering characteristics of the pipeline robot are investigated experimentally.

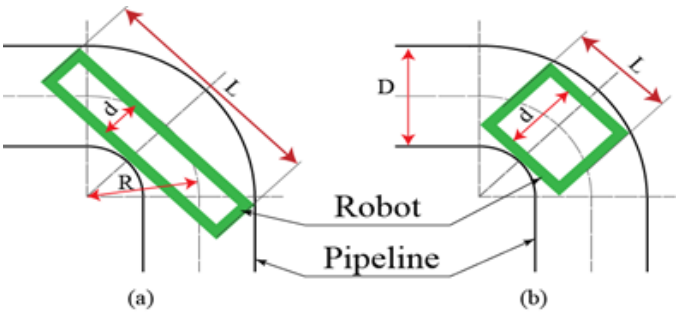

Fig. 6 *Two types of robots turning in pipeline*

The passability of the robot in curved pipes should consider the geometric dimensions of the robots and which simplify the robot into cylinder shaped. As shown in Fig. 6, there are two main two situation where the pipeline robot can be simplified into a cylindrical shape and the plan view is a rectangle. The first scenario is that the pipeline robot is in a "slender" shape as shown in Fig. 6 (a). During the process of passing through the elbow pipe, the end and tail of the robot are inside the straight pipe, and the middle part is inside the pipe elbow, which will "get stuck" in the pipe elbow due to its excessively long size. The second scenario is a "short thick" type as shown in Fig. 6 (b), where both the end and tail are located in the elbow pipe, but due to excessive size, they interfere with the pipeline and cannot pass through the elbow pipe. The robot size is determined by studying the diameter and length of the robot, as well as the diameter, angle, and radius of curvature of the pipeline. Assuming that the pipeline diameter is D, the curvature radius of the bend is R' (since the bend can be approximated as a circle, the curvature radius of the bend is equal to the radius of the central axis of the bend, i.e. R'=R), and the angle of the bend is assumed to be θ. The diameter and length of the robot are determined by d and L respectively. When the

Int. Journal of Integrated Engineering Vol. 16 No. 7 (2024) p. 300-312

robot is in the situation shown in Fig. 6 (a), the length and width of the robot should satisfy the following Equation 8:

$$\begin{cases} 0 < d < \left(R + \frac{D}{2}\right)\cos\frac{\theta}{2} - \left(R - \frac{D}{2}\right) \\ L_{max} = 2\left\{\left(R + \frac{D}{2}\right)\sin\frac{\theta}{2} + \left[\left(R + \frac{D}{2}\right)\cos\frac{\theta}{2} - \left(R - \frac{D}{2} + d\right)\right]\cot\frac{\theta}{2}\right\} \end{cases} \tag{8}$$

When the robot is in the situation shown in Fig. 6 (b), the length and width of the robot should satisfy the following Equation 9:

$$\begin{cases} \left(R + \frac{D}{2}\right)\cos\frac{\theta}{2} - \left(R - \frac{D}{2}\right) < d < D \\ L_{max} = 2\sqrt{\left(R + \frac{D}{2}\right)^2 - \left(R - \frac{D}{2} - d\right)^2} \end{cases} \tag{9}$$

Fig. 7 shows the experimental set up where the pipeline diameter and curvature radius are D = 400 mm and R= 600 mm respectively. R ≥ 1.5D and bend angle 0< θ< 90 ° are set for Fig. 6 (b) case. The minimum diameter of the pipeline robot during contraction is calculated to be 166mm < d < 400mm by using Equation 9. According to the Equation 9, L_{max} decreases with the increase of d. The range of L_{MAX} values is 0 < L_{max} < 1530mm. The minimum diameter of the reconfigurable robot during contraction is found to be d = 320 mm, and the length of the robot is L = 450 mm which is less than L_{MAX}. Therefore, it was found that proposed the pipeline robot meets geometric constraints and can pass through the pipeline smoothly.

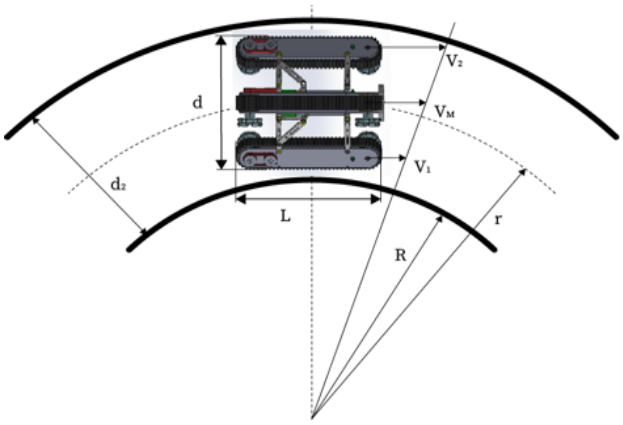

Fig. 7 *Schematic diagram of robot turning*

In addition to geometric constraints requirements, the robot should meet motion constraints as well. Due to the different positions of the driving wheels, the distance between the robot and the curvature of the elbow pipe is varied when the robot moves in a pipe. Therefore, it is necessary to adjust the speed of each driving wheel of the pipeline robot. To ensure that the pipeline robot passes through the pipe elbow smoothly, the outer driving wheel accelerates and the inner driving wheel decelerates.

The turning motion of a robot in a pipeline is achieved through the speed difference between two track wheels. To simplify the turning process of the robot, the center of the robot is always assumed to be at the center of the pipeline. As refer to Fig. 7, point *O* is the center of rotation, V_1、 and V_2 are the velocities of the inner and outer track wheels, V_M is the overall center of mass velocity, *r* is the turning radius of the robot's center of mass, *R* is the inner radius of the bend, and d_2 is the distance on both sides of the pipeline. *r* can be calculated as following Equation 10:

$$r = R + \frac{d_2}{2} \tag{10}$$

Using trigonometry principle, it can be concluded that $\frac{V_1}{V_M} = \frac{R}{R + \frac{d_2}{2}}$ (11) and $\frac{V_2}{V_M} = \frac{R + d_2}{R + \frac{d_2}{2}}$ (12)

Thus, the velocities of the inner, V_1 and outer, V_2 tracked wheels are:

$$\begin{cases} V_1 = V_M \dfrac{R}{R + \frac{d_2}{2}} \\ V_2 = V_M \dfrac{R + d_2}{R + \frac{d_2}{2}} \end{cases} \tag{13}$$

Equation 13 can be used to determine the velocities of the inner and outer track wheels of the robot when maneuver in different pipe diameters when the overall motion speed of the robot is known.

3. Results and Discussion

3.1 Motion Characteristics in Horizontal Pipe Simulation Test

The test is divided into three different scenarios as tabulated in Table 1.

Table 1 *Motion characteristics in horizontal pipe test scenarios*

No.	Time Frame	Scenarios
1	0～0.5 s	The robot is placed inside the pipeline and undergoes free fall motion
2	0.5～1.0 s	The motion of the robot's variable diameter mechanism enables the robot's driving module to adapt to the size of the inner wall of the pipeline
3	1～15s	Robot move in accordance with the pipeline's direction

The robot's motion trajectory in x and y axes and angular velocity measured along z-axis are depicted in Fig. 8,9,10 respectively. In Scenario 2 (0.5~1.0 s), there are significant displacements and angle deviations as the robot adjusting the tracked based on the size of the pipe. The robot's displacement change rate after adapting to the pipeline size (1-15 seconds) are 0.175% and 0.038% on the x and y axes respectively. Rotational angular velocity is relatively stable and reciprocating within a range of -2.7 to 1.7 °/s. The simulation results exhibit that the robot has good adaptability to pipeline sizes after the robot's pose is adaptively adjusted.

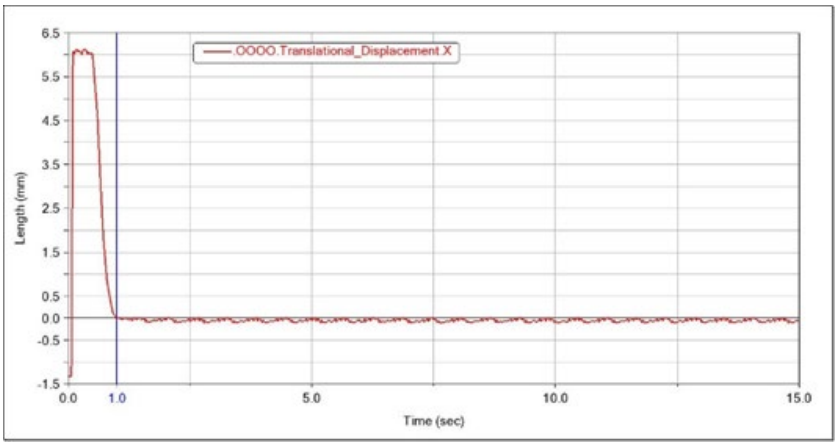

Fig. 8 *X-axis Centroid displacement*

Int. Journal of Integrated Engineering Vol. 16 No. 7 (2024) p. 300-312

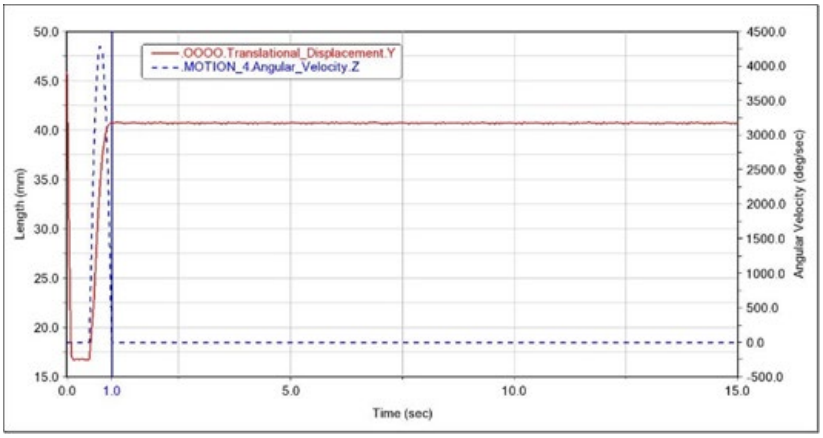

Fig. 9 *Y-axis Centroid displacement*

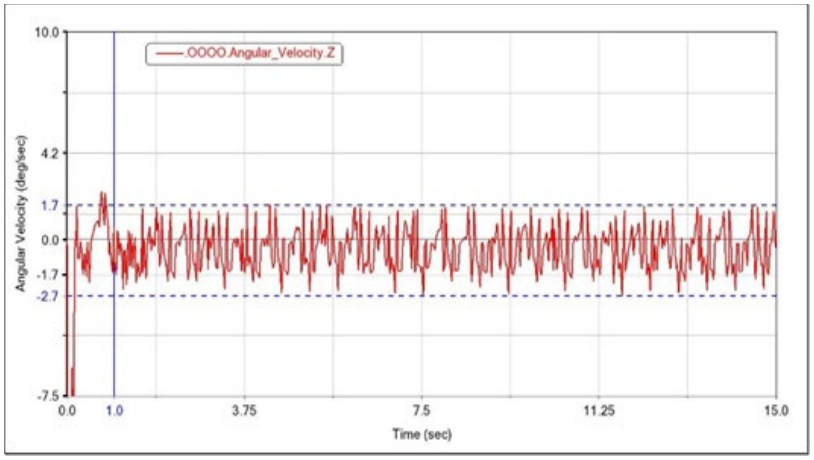

Fig. 10 *Z-axis angular velocity map of trajectory points*

3.2 Motion Characteristics in Elbow Pipe Simulation Test

The curved pipeline simulation is conducted in the Adams multibody dynamics simulation software. The simulation test is divided into three different scenarios as tabulated in Table 2.

Table 2 *Motion characteristics in elbow pipe test scenarios*

No.	Time Frame	Scenarios
1	0～0.3 s	The robot maintains a stationary state after free fall motion inside the pipeline.
2	0.3～2.0 s	The variable diameter mechanism of the robot is extended, allowing the robot drive module to adapt to the size of the inner wall of the pipeline
3	2.0～10.0s	The robot moves in a straight line along the direction of the pipeline
4	10.0～20.0s	The robot passes through a 90 ° curved pipeline
5	20.0～30.0s	The robot passes through a curved pipe and moves forward in a straight pipeline.

The robot is initially located at a certain distance from the pipeline's inner wall. Upon falling free (0.3-2.0s), the robot's angular velocity on the z-axis rapidly decreases to zero. The x-axis angular velocity of the robot exhibits significant vibration during the cornering stage (10-20s), whereas the y-axis angular velocity increases and then decreases. As soon as the robot passed through the curved pipeline (20-30s), it adapts its posture accordingly, and it runs smoothly. Fig. 11 – 13 show the simulation results in which it can be concluded that the pipeline robot is able to smoothly pass through 90° curved pipes.

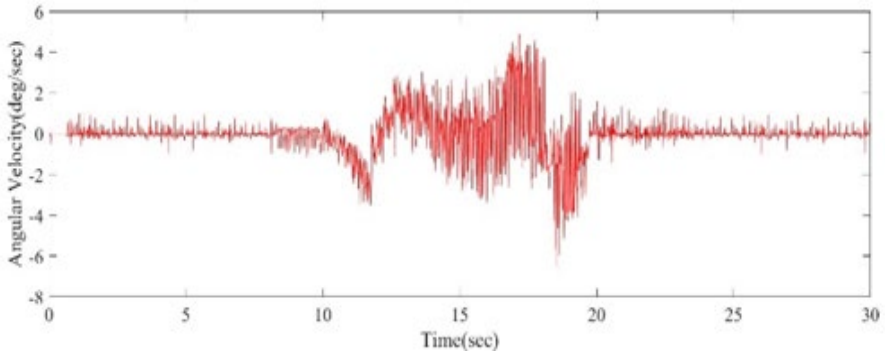

Fig. 11 *X-axis angular velocity*

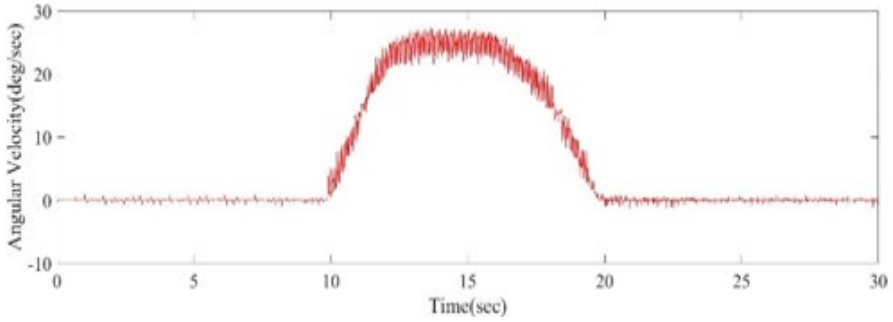

Fig. 12 *Y-axis angular velocity*

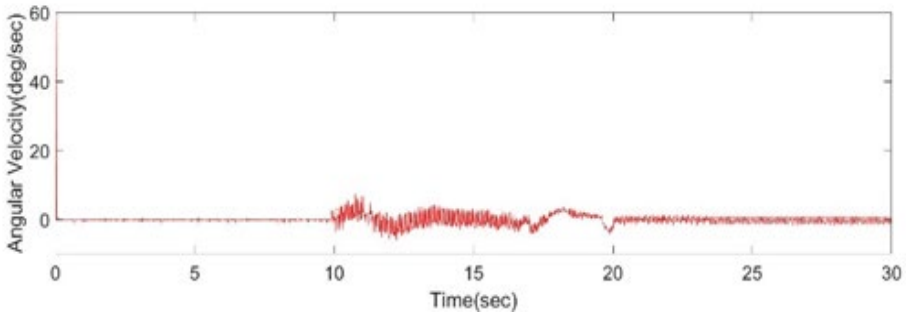

Fig. 13 *Z-axis angular velocity*

3.3 Adaptability Experiment of Robot Movement Inside Pipelines

Next, the developed robot is tested to maneuver in organic glass material pipe as shown in Fig. 14. This pipeline is made with a smooth interior and has a diameter of 320 mm and a length of 3 meters. Two experiment condition were conducted to investigate the adaptability of proposed mechanism in real world condition as follows:

- Horizontal pipeline experiment

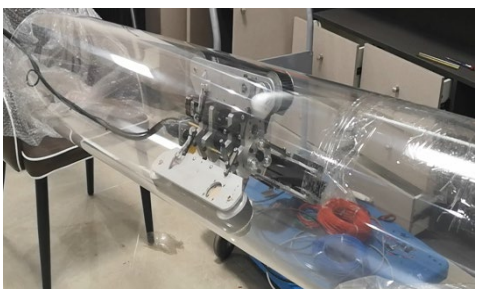

Fig. 14 *Horizontal pipeline experiment*

There are two driving modules on the bottom of the robot that contact the inner wall of the pipeline in the initial state, while the top driving module is not in contact with the inner wall. As the variable diameter mechanism extends, the robot's three sets of track modules are in full contact with the inner wall of the pipeline. Once the robot has adapted to the pipeline, it moves forward and backward continuously.

• 16 ° Slope Pipeline Experiment

Second test is conducted with the pipeline slopes of 16° as shown in Fig. 15. The robot is tested to move in the pipe forward and backward. It was found that the robot can perform the required movement smoothly.

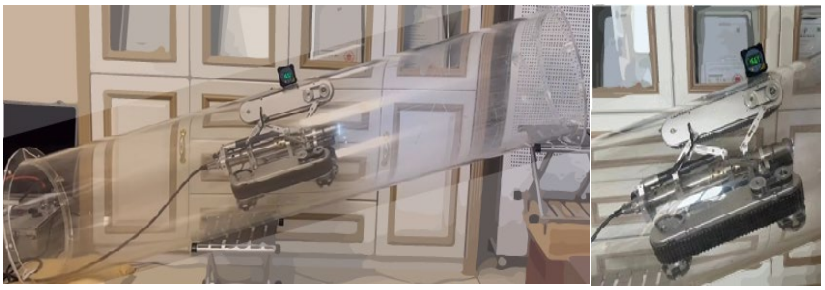

Fig. 15 *16° Slope Pipeline Experiment*

4. Conclusions

A detailed dynamic characteristics behavior of the developed pipeline robot is conducted to identify the required pressure, velocities and force for the robot to maneuver in the pipeline. It has been demonstrated that increasing the positive pressure of the driving module to the pipe wall by expanding the variable diameter mechanism increases the effective traction force, which increases the stability of the robot's movement. The robotic system can quickly adapt to circular pipes within its own diameter range, which makes it suitable for the horizontal installation of circular pipes as well as the installation of circular pipes on a slope. During the posture adjustment stage, the robot undergoes self-rotation inside a circular pipeline installed horizontally or at a certain angle. With the robot adapted to the inner wall of the circular pipeline, the robot is capable of moving forward and backward steadily inside the pipeline, indicating that this type of robot has good motion adaptability to circular pipelines installed horizontally and at a specified slope.

The hardware and software for this pipeline robot have been developed successfully and can maneuver in bend pipe as well. The developed driving modules are capable to control of forward, backward, and climbing robot movements. Future work will explore implementation of visual based approach to detect pipeline defects autonomously using embedded neural networks.

Acknowledgement

This work was supported by Universiti Teknologi MARA, Toyohashi University of Technology (International Grant 100-TNCPI/INT 16/6/2 (057/2023) and Shaanxi Polytechnic Institute (2023YKZX-004). We express our gratitude to the UiTM-TUT collaboration lab for providing some resources for the experiment.

Conflict of Interest

Authors declare that there is no conflict of interests regarding the publication of the paper.

Author Contribution

The authors confirm contribution to the paper as follows: ***study conception and design:*** *Jia Chaoyu; Chen Pengwei;* ***data collection:*** *Jia Chaoyu; Wan Nurshazwani Wan Zakaria;* ***analysis and interpretation of results:*** *Jia Chaoyu; Wan Nurshazwani; Chen Pengwei; Mohd Nor Azmi Ab Patar; Mohd Razali Md Tomari;* ***draft manuscript preparation:*** *Jia Chaoyu; Wan Nurshazwani; Chen Pengwei; Mohd Nor Azmi Ab Patar; Mohd Razali Md Tomari;* ***Manuscript review and intellectual content:*** *Wan Nurshazwani Wan Zakaria; Mohd Nor Azmi Ab Patar;* ***conceptualization, research methodology, and supervision:*** *All authors reviewed the results and approved the final version of the manuscript.*

References

[1] Ho, M., El-Borgi, S., Patil, D., & Song, G. (2020). Inspection and monitoring systems subsea pipelines: A review paper. *Structural Health Monitoring*, *19*(2), 606-645, https://doi.org/10.1177/1475921719837718

[2] Verma, A., Kaiwart, A., Dubey, N. D., Naseer, F., & Pradhan, S. (2022). A review on various types of in-pipe inspection robot. *Materials Today: Proceedings*, *50*, 1425-1434, https://doi.org/10.1016/j.matpr.2021.08.335
[3] Colvalkar, A., Pawar, S. S., & Patle, B. K. (2023). In-pipe inspection robotic system for defect detection and identification using image processing. *Materials Today: Proceedings*, 72, 1735-174, https://doi.org/10.1016/j.matpr.2022.09.476
[4] Ab Rashid, M. Z., Yakub, M. F. M., bin Shaikh Salim, S. A. Z., Mamat, N., Putra, S. M. S. M., & Roslan, S. A. (2020). Modeling of the in-pipe inspection robot: A comprehensive review. *Ocean Engineering*, *203*, 107206, https://doi.org/10.1016/j.oceaneng.2020.107206
[5] Rayhana, R., Yun, H., Liu, Z., & Kong, X. (2023). Automated defect-detection system for water pipelines based on CCTV inspection videos of autonomous robotic platforms. *IEEE/ASME Transactions on Mechatronics*, https://doi.org/10.1109/TMECH.2023.3307594
[6] Ma, Q., Tian, G., Zeng, Y., Li, R., Song, H., Wang, Z., Gao, B. and Zeng, K. (2021). Pipeline in-line inspection method, instrumentation and data management. *Sensors*, *21*(11), 3862, https://doi.org/10.3390/s21113862
[7] Kazeminasab, S., Sadeghi, N., Janfaza, V., Razavi, M., Ziyadidegan, S., & Banks, M. K. (2021). Localization, mapping, navigation, and inspection methods in in-pipe robots: A review. *IEEE Access*, *9*, 162035-162058, https://doi.org/10.1109/ACCESS.2021.3130233
[8] Le, D. V. K., Chen, Z., & Rajkumar, R. (2020). Multi-sensors in-line inspection robot for pipe flaws detection. *IET Science, Measurement & Technology*, *14*(1), 71-82, https://doi.org/10.1049/iet-smt.2019.0171
[9] Rayhana, R., Jiao, Y., Liu, Z., Wu, A., & Kong, X. (2020). Water pipe valve detection by using deep neural networks. *Proceedings SPIE 11382: Smart Structures and NDE for Industry 4.0, Smart Cities, and Energy Systems*, *USA, 1138205,* https://doi.org/10.1117/12.2558886
[10] Yin, X., Chen, Y., Bouferguene, A., Zaman, H., Al-Hussein, M., & Kurach, L. (2020). A deep learning-based framework for an automated defect detection system for sewer pipes. *Automation in Construction*, *109*, 102967, https://doi.org/10.1016/j.autcon.2019.102967
[11] Bogdan, P. A., Wheadon, J., Klein, F. B., & Gianni, M. (2021, August). Magnetic tracked robot for internal pipe inspection. *2021 European Conference on Mobile Robots (ECMR), 1-6,* https://doi.org/10.1109/ECMR50962.2021.9568790
[12] Li, H., Li, R., Zhang, J., & Zhang, P. (2020). Development of a pipeline inspection robot for the standard oil pipeline of China national petroleum corporation. *Applied Sciences*, *10*(8), 2853, https://doi.org/10.3390/app10082853
[13] Liu, X., Song, M., Fang, Y., Zhao, Y., & Cao, C. (2022). Worm-inspired soft robots enable adaptable pipeline and tunnel inspection. *Advanced Intelligent Systems*, *4*(1), 2100128, https://doi.org/10.1002/aisy.202100128
[14] Guanhua, F. E. N. G., Wenhao, L. I., Zhang, H., Zhigang, L. I., & Zhen, H. E. (2020). Development of a wheeled and wall-pressing type in-pipe robot for water pipelines cleaning and its traveling capability. *Mechanics*, *26*(2), 134-145, https://doi.org/10.5755/j01.mech.26.2.18783
[15] Kim, H. M., Choi, Y. S., Lee, Y. G., & Choi, H. R. (2016). Novel mechanism for in-pipe robot based on a multiaxial differential gear mechanism. *IEEE/ASME Transactions on Mechatronics*, *22*(1), 227-235, https://doi.org/10.1109/TMECH.2016.2621978
[16] Tourajizadeh, H., Rezaei, M., & Sedigh, A. H. (2018). Optimal control of screw in-pipe inspection robot with controllable pitch rate. *Journal of Intelligent & Robotic Systems*, *90*, 269-286, https://doi.org/10.1007/s10846-017-0658-7
[17] Yan, H., Wang, L., Li, P., Wang, Z., Yang, X., & Hou, X. (2020). Research on passing ability and climbing performance of pipeline plugging robots in curved pipelinzes. *IEEE Access*, *8*, 173666-173680, https://doi.org/10.1109/ACCESS.2020.3025560
[18] Abidin, A. S. Z., Chie, S. C., Zaini, M. H., Pauzi, M. F. A. M., Sadini, M. M., Mohamaddan, S., Jamali, A., Muslimen, R., Ashari, M. F., & Jamaludin, M. S. (2017). Development of in-pipe robot D300: Cornering mechanism. *MATEC Web of Conferences 87, 02029,* https://doi.org/10.1051/matecconf/20178702029
[19] Zhao, W., Zhang, L., & Kim, J. (2020). Design and analysis of independently adjustable large in-pipe robot for long-distance pipeline. *Applied Sciences*, *10*(10), 363, https://doi.org/10.3390/app10103637

[20] Yeh, T. J., & Weng, T. H. (2021). Analysis and control of an in-pipe wheeled robot with spiral moving capability. *Journal of Autonomous Vehicles and Systems*, *1*(1), 011002, https://doi.org/10.1115/1.4048376
[21] Kazeminasab, S., Akbari, A., Jafari, R., & Banks, M. K. (2021, March). Design, characterization, and control of a size adaptable in-pipe robot for water distribution systems. *2021 22nd IEEE International Conference on Industrial Technology (ICIT)*, 39-46, https://doi.org/10.1109/ICIT46573.2021.9453583
[22] Gharib, M., Alnouri, L., Alsulaiti, A., Buhendi, I., & Al-Hamidi, Y. (2020, November). Development of a novel modular robot for vertical pipeline climbing. *ASME International Mechanical Engineering Congress and Exposition,* 84553, V07BT07A010, https://doi.org/10.1115/IMECE2020-23163
[23] Shah, D., Dave, J., Majithiya, A., & Patel, Y. (2021, November). Conceptual design and analysis of pipe climbing robot. *Journal of Physics: Conference Series,* 2115(1), 012004, https://doi.org/10.1088/1742-6596/2115/1/012004